Nuclear medicine nanotechnology: Reilly reviews the development of carbon nanotubes and looks at the benefits and risks associated with initial in vivo applications in tumor targeting and drug delivery. . . . . ***Page 1039***

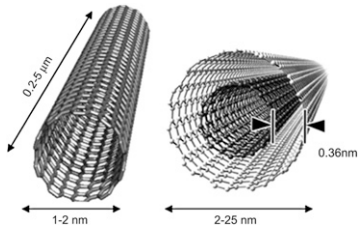

Looking for stunning: Silberstein compares outcomes of ablative radioiodine therapy after diagnostic studies with ^{123}I or ^{131}I to determine whether diagnostic dosages reduce the efficacy of postthyroidectomy remnant ablation. . . . . ***Page 1043***

Heterogeneity of low-grade gliomas: Wyss and colleagues use ^{18}F-FET PET in low-grade gliomas to assess cerebral blood flow and microvessel density characteristics, essential elements in understanding and developing advanced chemotherapeutic approaches. . . . . ***Page 1047***

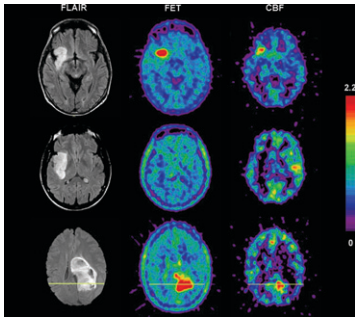

PET/CT in Crohn's disease: Louis and colleagues investigate the efficacy of combined functional/anatomic imaging in the noninvasive localization and characterization of gastrointestinal tract lesions in patients with Crohn's disease. . . . . ***Page 1053***

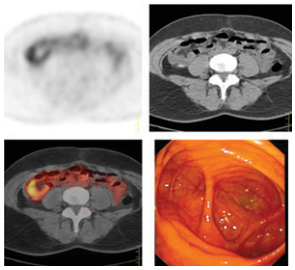

Error correction in cardiac PET/CT: Büther and colleagues evaluate 2 methods of thresholding CT data to correct for contrast media–related artifacts that impair PET quantification of tracer uptake in cardiac PET/CT imaging. . . . ***Page 1060***

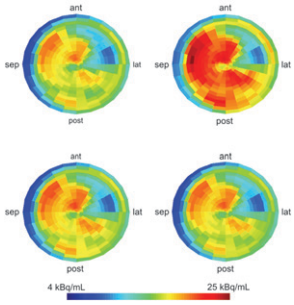

PET MPI in cardiac disease management: Merhige and colleagues detail the costs and clinical outcomes, including revascularization rates, in groups of patients undergoing ^{82}Rb PET myocardial perfusion imaging (MPI) and SPECT MPI for coronary artery disease. . . . . ***Page 1069***

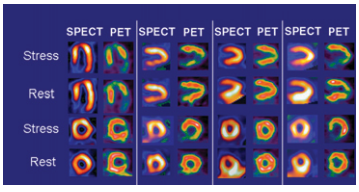

Brown fat in pheochromocytomas: Hadi and colleagues review ^{18}F-fluorodopamine and ^{18}F-FDG PET/CT images in patients with known or suspected pheochromocytomas to determine whether typical patterns of localized uptake associated with brown adipose fat can be identified. . . . . ***Page 1077***

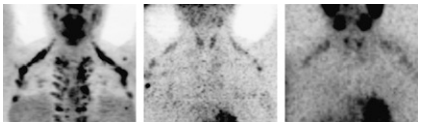

SPECT/CT parathyroid scintigraphy: Lavely and colleagues compare SPECT/CT, SPECT, and planar imaging in patients with primary hyperparathyroidism and investigate whether localization is improved by dual-phase acquisition in these 3 modalities. . . . . ***Page 1084***

Registration strategies in cardiac SPECT/CT: Goetze and colleagues focus on the role of misregistration in SPECT/CT in a database of more than 100 patients undergoing myocardial perfusion imaging and assess the performance of a software-based approach for reregistration. . . . . ***Page 1090***

Early outcomes after CABG: Wu and colleagues compare the abilities of contrast-enhanced MRI and ^{18}F-FDG PET/^{201}Tl SPECT to assess myocardial viability and predict early functional outcome in patients undergoing coronary artery bypass graft surgery. . . . . ***Page 1096***

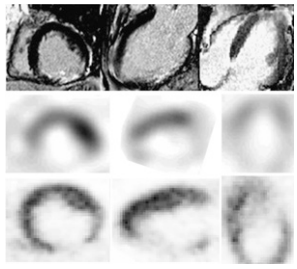

Predicting CRT response: Henneman and colleagues investigate whether the degree of left ventricular dyssynchrony as assessed by gated myocardial perfusion SPECT can predict which patients with severe heart failure will respond to cardiac resynchronization therapy. . . . ***Page 1104***

Cardiac PET/CT artifacts: Gould and colleagues report on causes, results, and corrective approaches in misregistration of helical CT attenuation and emission PET images in patients undergoing PET/CT myocardial perfusion imaging. . . . . ***Page 1112***

^{82}Rb PET/CT myocardial database: Santana and colleagues describe the development and validation of a normal database and criteria for abnormality for rest–stress ^{82}Rb PET/CT myocardial perfusion imaging and highlight the research potential of such a resource. . . . . ***Page 1122***

Normative early AD references: Mosconi and colleagues explore the utility of an ^{18}F-FDG PET database of longitudinally confirmed healthy elderly individuals in improving the diagnosis of Alzheimer's disease and mild cognitive impairment. . . . . ***Page 1129***

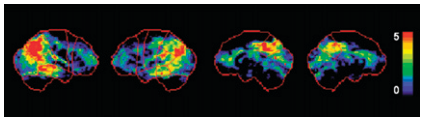

Viability in heart failure: Schinkel and colleagues provide an educational overview of current noninvasive techniques for assessing myocardial viability in patients with chronic ischemic left ventricular dysfunction. . . . . ***Page 1135***

Modulation of brain function in Parkinson's: Pellegrino and colleagues describe the PET imaging profile and expression of dopaminergic and metabotropic glutamate receptors in a parkinsonian rodent model, with resulting data that offer insights into the mechanisms of neurodegeneration. . . . . ***Page 1147***

Better brain imaging: Ryu and colleagues use ^{18}F-FCWAY, a PET radioligand for imaging serotonin receptor imaging, to test the ability of disulfiram to inhibit defluorination in humans. . . . . ***Page 1154***

Targeting tumor angiogenesis: Li and colleagues report on the development of and initial studies with ^{64}Cu-labeled multimeric RGD peptides for PET imaging of tumor integrin $\alpha_v\beta_3$ expression. . . . . ***Page 1162***

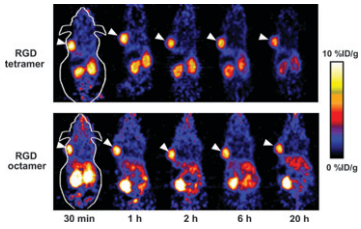

Angiogenesis imaging: Rossin and colleagues describe the use of a ^{76}Br-labeled fibronectin-binding human antibody derivative and small-animal PET to image the extra domain B of fibronectin, an angiogenesis-related target in solid tumors. . . . ***Page 1172***

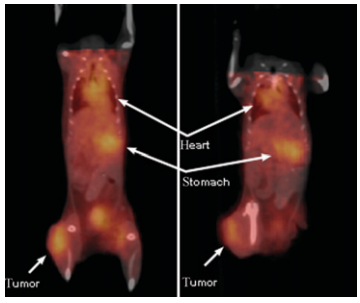

Tumor targeting with carbon nanotubes: McDevitt and colleagues detail the synthesis and in vitro and in vivo evaluation of novel prototype nanostructures consisting of biologics, radionuclides, fluorochromes, and carbon nanotubes as molecular-level drug delivery platforms. . . . . ***Page 1180***

Radiolytic effects of ^{211}At: Pozzi and Zalutsky offer the third in a series on targeted radiopharmaceutical chemistry, focusing on the effect of radiation dose before initiation of labeling and the potential results on the efficiency of α-emitter radiopharmaceutical synthesis. . . . . ***Page 1190***

Microvolumetric blood counter: Convert and colleagues describe the development and evaluation of an automated β-particle blood counter designed to circumvent the limitations of manual sampling in small-animal PET imaging by measuring blood activity in real time. . . . . ***Page 1197***

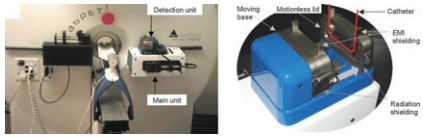

Imaging glutamate receptors: Treyer and colleagues evaluate different methods for analysis of human data acquired using ^{11}C-ABP688, a novel PET ligand that targets the subtype 5 metabotropic glutamate receptor. . . . . ***Page 1207***

Assessing peripheral arterial occlusive disease: Peñuelas and colleagues investigate the utility of ^{13}N-ammonia small-animal PET imaging for semiquantitative evaluation of hindlimb perfusion in mouse models of acute hindlimb ischemia. . . . . ***Page 1216***

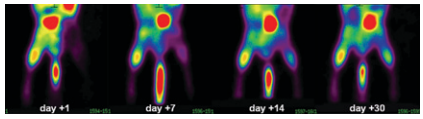

ON THE COVER

Cardiac PET/CT is rapidly expanding despite false-positive results due to misregistration. Averaged cine data acquired during normal breathing can be applied using reconstruction software or visual shifting to eliminate artifactual defects. Properly coregistered PET/CT data provide perfusion images suitable for assessing coronary artery disease.

See page 1117.